Cesca, S., Heimann, S., Kriegerowski, M., Saul, J., Dahm, T. (2017): Moment Tensor Inversion for Nuclear Explosions: What can we learn from the 6 January and 9 September 2016 Nuclear Tests, North Korea? - *Seismological Research Letters*, *88*, 2A, pp. 300—310.

DOI: http://doi.org/10.1785/0220160139

THE SEISMOLOGICAL SOCIETY OF AMERICA
400 Evelyn Ave., Suite 201
Albany, CA 94706-1375
(510) 525-5474; FAX (510) 525-7204
www.seismosoc.org

Moment Tensor Inversion for Nuclear Explosions: What Can We Learn from the 6 January and 9 September 2016 Nuclear Tests, North Korea?

by Simone Cesca, Sebastian Heimann, Marius Kriegerowski, Joachim Saul, and Torsten Dahm

ABSTRACT

Two nuclear explosions were carried out by the Democratic People's Republic of North Korea in January and September 2016. Epicenters were located close to those of the 2006, 2009, and 2013 previous explosions. We perform a seismological analysis of the 2016 events combining the analysis of full waveforms at regional distances and seismic array beams at teleseismic distances. We estimate the most relevant source parameters, such as source depth, moment release, and full moment tensor (MT). The best MT solution can be decomposed into an isotropic source, directly related with the explosion and an additional deviatoric term, likely due to near-source interactions with topographic and/or underground facilities features. We additionally perform an accurate resolution test to assess source parameters uncertainties and trade-offs. This analysis sheds light on source parameters inconsistencies among studies on previous shallow explosive sources. The resolution of the true MT is hindered by strong source parameters trade-offs, so that a broad range of well-fitting MT solutions can be found, spanning from a dominant positive isotropic term to a dominant negative vertical compensated linear vector dipole. The true mechanism can be discriminated by additionally modeling first-motion polarities at seismic arrays at teleseismic distances. A comparative assessment of the 2016 explosion with earlier nuclear tests documents similar vertical waveforms but a significant increase of amplitude for the 2016 explosions, which proves that the 9 September 2016 was the largest nuclear explosion ever performed in North Korea with a magnitude M_w 4.9 and a shallow depth of less than 2 km, although there are no proofs of a fusion explosion. Modeling transversal component waveforms suggests variable size and orientation of the double-couple components of the 2009, 2013, and 2016 sources.

Electronic Supplement: Results of simulated annealing moment tensor (MT) inversion using a synthetic dataset, and a table of amplitude correction coefficients for each station used for the MT inversion.

INTRODUCTION

On 6 January 2016, 01:30:01.1 UTC, an m_b 5.1 nuclear explosion test was carried out at 129.07° E, 41.31° N (GEOFON real-time bulletin, see Data and Resources) by the Democratic People's Republic of Korea (DPRK) in its North Hamgyong Province. The country government announced the successful experiment of a hydrogen bomb after the explosion, through a communication on official state media. A second explosion (m_b 5.3 according to GEOFON) was carried out on 9 September 2016. These tests follow the previous blasts in 2006, 2009, and 2013. The DPRK hydrogen bomb claim can be hardly debated on a seismological basis, but the seismic signals recorded at regional and teleseismic distances can be used to assess the location, depth, magnitude, and focal mechanism.

Seismic signals produced by explosions of various nature can be analyzed using seismological tools to determine epicentral location, depth, and moment release estimate, and/or to discriminate explosive sources from natural shallow seismicity. The discrimination of energetic nuclear explosions can take advantage of regional moment tensor (MT) inversion methods, through the resolution of strong isotropic components. The full seismic MT (Gilbert, 1971) is thus a valuable model for such applications, because it accounts for shear, tensile, and isotropic source radiation pattern, under a point-source approximation. The MT inversion itself remains, however, challenging for signals generated by shallow sources of moderate magnitude. To overcome limitations in modeling high-frequency signals, affected by poorly modeled local scale structural heterogeneities, MT inversion approaches attempt to model low-frequency radiation only. However, this decreases the resolution of certain MT components. Because of the poor

 doi: 10.1785/0220160139

resolution of the isotropic component (Kawakatsu, 1996; Dufumier and Rivera, 1997; Shuler *et al.*, 2013), often only deviatoric MTs are considered. Such an approach is not adequate for explosion source. Further ambiguities among MT configurations were discussed by Shuler *et al.* (2013), concerning isotropic and horizontal tensile crack solutions of different signs, but also concerning pure deviatoric MTs, involving compensated linear vector dipoles (CLVDs) and double couples (DCs) with different orientations (Bukchin *et al.*, 2010). Beside the uncertainties of MT components arising for certain types of observations (Kawakatsu, 1996; Dufumier and Rivera, 1997) or in case of poor monitoring conditions (e.g., Domingues *et al.*, 2013), further ambiguities in the MT interpretation may arise from the adopted MT decomposition. The full MT decomposition into isotropic and deviatoric components is unique, but the decomposition of the deviatoric term is not (the standard one is by CLVD and DC with a common axis; see Jost and Hermann, 1989; Minson and Dreger, 2008). Recent interpretations of collapse events in mining (Rudzinski *et al.*, 2016) and volcanic (Heimann *et al.*, 2015) environments illustrate potential interpretation pitfalls due to the standard MT decomposition.

MT inversion for the 2009 North Korea explosion using different constrains (Ford *et al.*, 2009) is illustrative of the MT inversion challenges. The authors applied a time-domain MT inversion algorithm modeling regional waveforms in the 0.02–0.10 Hz frequency range. Results, obtained assuming a full MT, a deviatoric MT, a DC, or a pure isotropic source model, are extremely different, both in terms of the source geometry of each MT component, their seismic moment, the orientation of the DC, and the overall scalar moment and magnitude. These differences were further widened by Barth (2014), who discussed the seismic source of the 2009 and 2013 explosion. Beside their close epicenters (Wen and Long, 2010; Zhang and Wen, 2013), their common origin (shallow nuclear explosions), and the adoption of comparable full waveform-based inversion techniques, the results were quite different. Both authors derived a dominant positive isotropic component, but solutions strongly differed in terms of the deviatoric term. According to the full MT solution of Ford *et al.* (2009), the deviatoric component of the 2009 explosion (S. Ford, personal comm., 2016) was composed of an east-southeast–west-northwest-oriented thrust faulting (strike 107°, dip 77°, and rake 88°) and a positive CLVD. Under the same approximation, Barth (2014) attributed the deviatoric components of both the 2009 and 2013 explosions to a northeast–southwest normal fault DC, plus a negative subvertical CLVD. A potential reason for the discrepancy in former solutions may be found in the different adopted velocity models. Barth (2014) assumed a smooth 3D velocity model; this attempt, potentially valuable, apparently did not significantly improve the MT resolution, because the difference among synthetics generated for 1D and 3D models were said to be minor. Therefore, the use of 3D Green's functions is unlikely the only reason behind the discrepancy among full MT solutions by Ford *et al.* (2009) and Barth (2014).

In this work, we aim to assess the MT, scalar moment, centroid location, and depth of the 2016 nuclear explosions. Furthermore, we make use of waveform similarity technique to discuss the source properties in a comparative approach, taking as reference the waveforms from the 2009 and 2013 explosions and their published models. To improve our resolution, we combine the regional full-waveform MT inversion with array techniques applied at teleseismic distances (a data overview is given in Fig. 1).

LOCATION AND RELATIVE SCALAR MOMENTS

The GEOFON bulletin provides a first reference location (129.07° E, 41.31° N) and magnitude estimates of m_b 5.1 and 5.3, for the January and September 2016 explosions, respectively. Catalog depths are fixed to 1 km, a default value due to limited depth resolution for shallow sources. The location site is in the vicinity of the previous blast locations, according to Ford *et al.* (2009) and Barth (2014). Displacement records are obtained upon instrument restitution, demean, detrend, and downsampling to 2 s; we improve the restitution procedure by empirical determination of amplitude correction factors (see the Ⓔ electronic supplement to this article for procedure details and a list of scaling coefficients). Data are high-pass filtered above 0.01 Hz. We follow the same procedure for the 2009 and 2013 events and compare selected good-quality traces with recordings available for the three explosion events (Fig. 2). Regional seismic signals are characterized by dominant Rayleigh waves and less energetic but not negligible Love waves. A very high waveform similarity among the signals is found for vertical and radial components in the frequency bands 0.02–0.05 Hz and 0.033–0.10 Hz. The comparison of the lower-frequency radiation qualitatively confirms the radial symmetry of the radiation pattern; a similar comparison in the frequency range up to 0.1 Hz starts to depict lateral heterogeneity of the crustal structure anomalies, with shorter higher-amplitude waveforms recorded at stations toward northwest and longer but weaker surface waves in the opposite direction.

The large similarity with waveforms produced by previous nuclear explosion provides a first, strong indication toward the presence of a dominant isotropic source component also for the 2016 events. We rely on the waveforms similarity to estimate a relative magnitude for the January 2016 explosion, having the magnitudes estimated for the 2009 and 2013 explosions as a reference. Scalar moments for the January 2016 event are estimated multiplying the reference scalar moments of previous explosions by the median scaling coefficients among vertical waveforms recorded at seven common stations, revealing that the moment released by the 2013, January 2016, and September 2016 explosions were, respectively, 1.87, 2.38, and 3.44 times larger with respect to the 2009 explosion. We first consider the 2009 explosion as a reference, for which Ford *et al.* (2009) estimated scalar moments of 1.8×10^{15} N·m (isotropic model), 3.6×10^{15} N·m (isotropic term of the full MT), and 6.3×10^{15} N·m (full MT); considering the range of relative amplitudes of vertical traces at different stations, we can

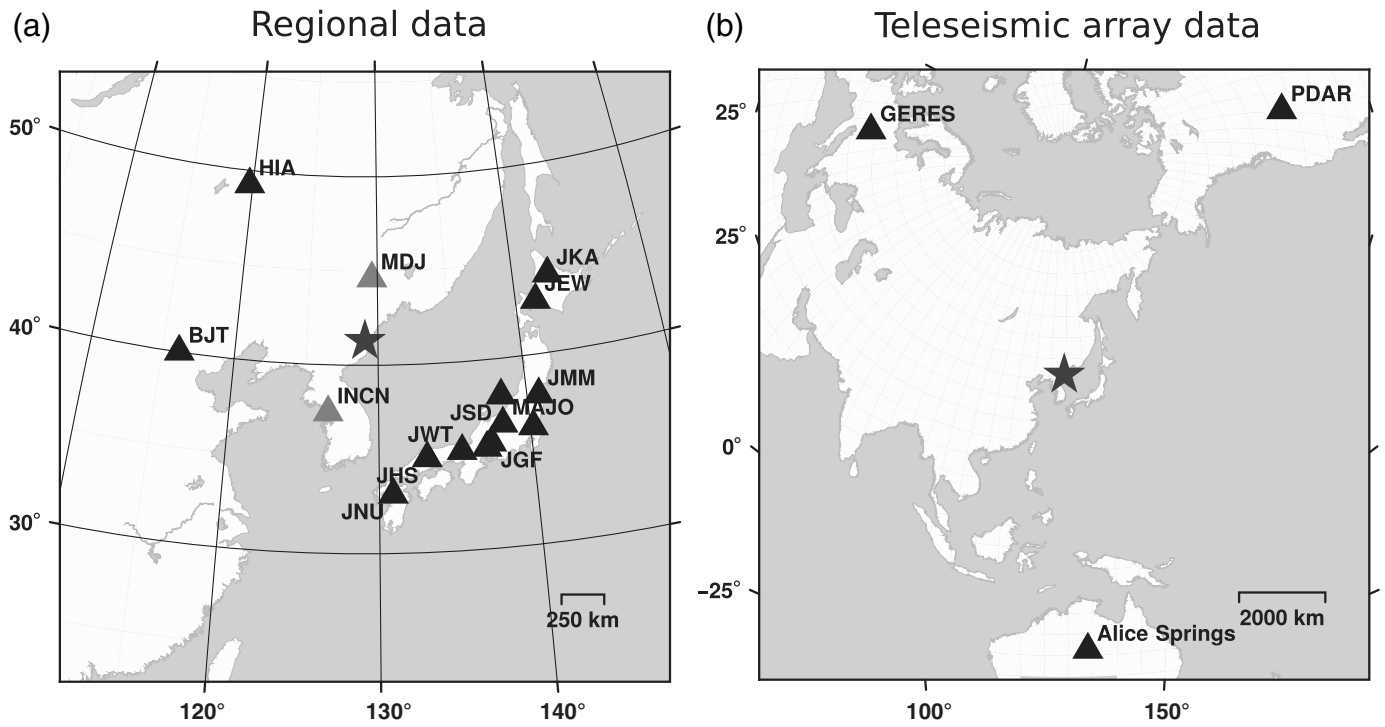

▲ **Figure 1.** Overview of the seismic data used in this study to investigate the source processes of the 2016 nuclear test, Democratic People's Republic of Korea (DPRK, star). (a) Regional data used for moment tensor (MT) inversion (gray triangles for stations at less than 600-km epicentral distances and black triangles for further stations up to 1200-km epicentral distance). (b) Location of the seismic arrays at teleseismic distances used to model the *P*-wave beam.

estimate for the 2016 event a scalar moment between 4.3×10^{15} and 1.5×10^{16} N·m (M_w 4.4–4.8). Barth (2014) estimated for the 2009 event a larger scalar moment of 2.2×10^{16} N·m (1.1×10^{16} N·m, when considering only the isotropic contribution); relying on these range of values, we come to larger estimates in the range $2.6–5.2 \times 10^{16}$ N·m (M_w 4.9–5.1) for the January 2016 event. The scalar moment comparison relied on the relative amplitudes of vertical components, which are in large measure controlled by the isotropic term. Transversal components are of interest here to discuss the radiation pattern of the deviatoric term. Figure 2a (right) shows a high similarity among transversal component waveforms, but it also depicts different amplitude ratios at different stations, which are only explained by differences among the DC mechanisms of different events. This anomalous pattern is so outstanding that largest amplitudes of transversal components are found for the 2013 and September 2016 events, whereas the September 2016 event generated the largest vertical signals. This observation supports the inference (Barth, 2014) of a stronger release of shear energy for the 2013 event; however, DC terms of the 2009 and 2013 events should have a different orientation, because scaling factors differ significantly at different stations.

OVERVIEW ON MT INVERSION RESULTS FOR NORTH KOREAN EXPLOSIONS

A wide panorama of MT inversion algorithms is nowadays available (see a review in Cesca and Grigoli, 2015), some of them accounting for isotropic source components. For the analysis of previous explosions in North Korea, Ford *et al.* (2009) and Barth (2014) followed a full-waveform approach, beside referring to different algorithm implementations: Ford *et al.* (2009) solved the inverse problem in the time domain and Barth (2014) fit both amplitude and phase spectra (Barth *et al.*, 2007). A useful alternative, given the experienced challenges in modeling seismic traces in the time domain with a single velocity model (Ford *et al.*, 2009), is to perform an amplitude spectra MT inversion (Cesca *et al.*, 2013). Following this approach, we fit the amplitude spectra of full waveforms in the 0.02–0.04 Hz frequency band; the amplitude spectra inversion is less dependent on precise waveform modeling and alignment. The time-domain approach is only used for the closest stations (below 600 km) to constrain the MT polarity. To test the robustness of the MT inversion, we repeat the inversion assuming three different crustal velocity models, upon a common ak135 mantle model (Kennett *et al.*, 1995). The three velocity models are the one provided by the CRUST 2.0 (Bassin *et al.*, 2000) database for the epicentral region, its simplified implementation using a homogeneous crust with average velocities, and the MDJ2 model of Ford *et al.* (2009). The epicenter is fixed according to the GEOFON bulletin. The inversion is iterated in the 0.5–2.0 km depth range, with a depth grid of 0.5 km, and further refined to 0.1 km in the 1.5–2.0 km range, at which best-fitting solutions are found.

We first discuss the January 2009 explosion. The best fit (Fig. 3) is found for the velocity model MDJ2 for at a depth

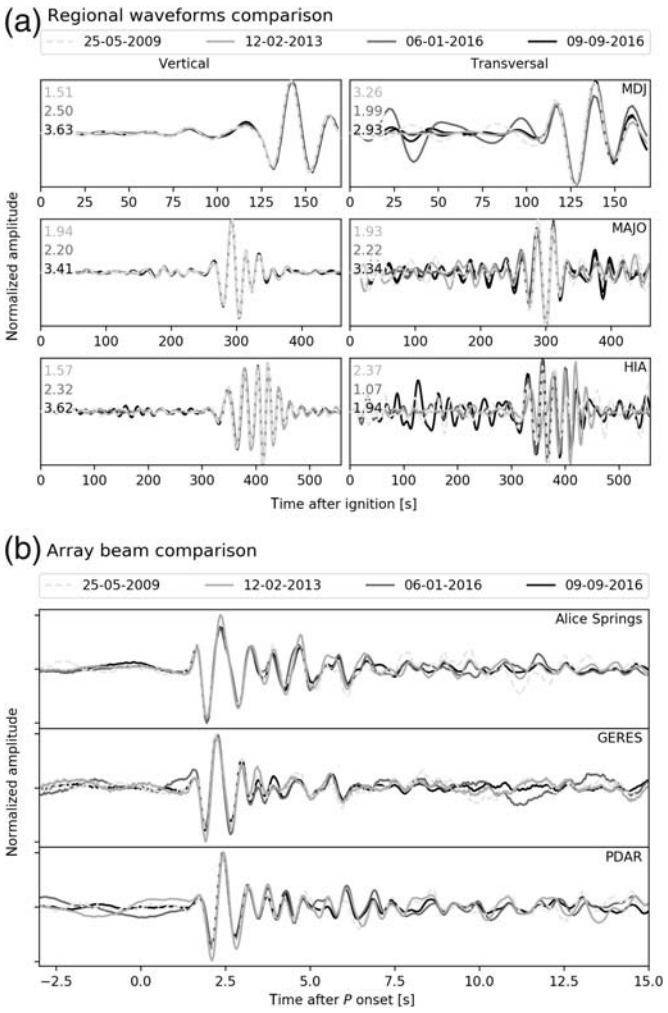

▲ **Figure 2.** Waveform comparison among the 2016 explosions and previous tests in 2009 and 2013, according to the legend. (a) The comparison of regional full waveforms for selected vertical and transversal components in the 0.02–0.05 Hz frequency range depicts the high waveform similarity. Numbers indicate the waveform amplitude scaling coefficients for the 2013, January 2016, and September 2016 explosions, with respect to the 2009 one. (b) A similar plot illustrates the similarity of vertical-component *P*-wave beams at selected seismic arrays (filtered in the 1–6 Hz frequency band).

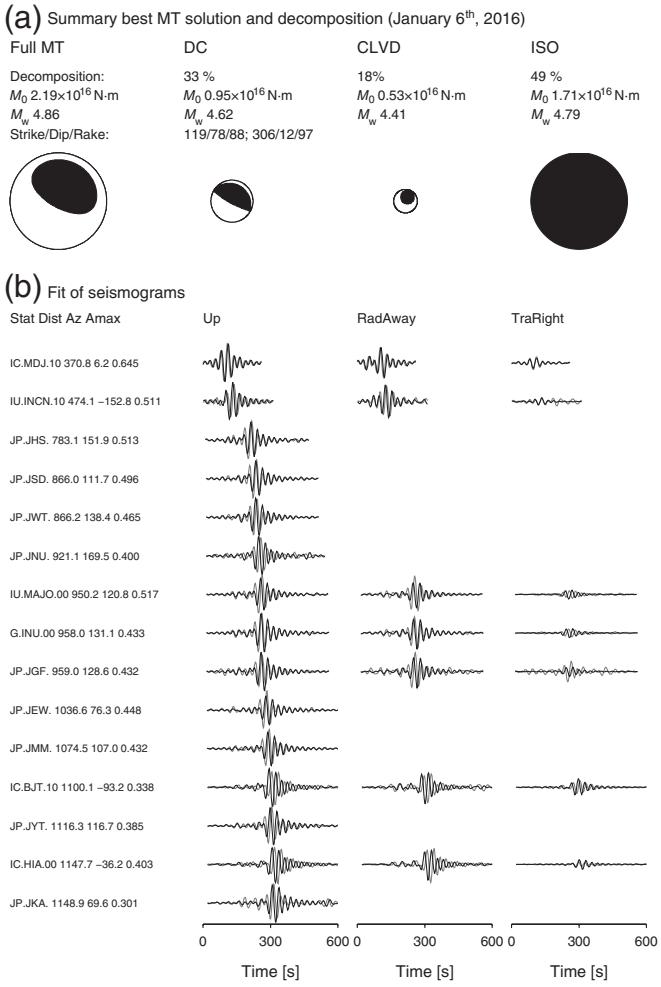

▲ **Figure 3.** MT inversion results for the 6 January 2016 explosion. (a) Summary of the best MT result out of the regional full-waveform amplitude spectra (up to 1200 km distance) MT inversion, with the polarity and centroid location constrained upon full-waveform displacements (up to 600 km distance). The plot reports the focal sphere of the full MT and decomposed terms, according to the standard decomposition, scalar moment, moment magnitudes, and orientation of the double-couple (DC) focal planes. (b) Fit of displacement traces in the time domain for the best MT solution. Synthetics are denoted by black thin lines, observations by gray thick lines. The network, station, location codes, the distances (km), the azimuth (°), and the maximal amplitudes (10^{-6} m) are reported at the left side. Traces are normalized according to the maximal amplitude at each station to highlight the amplitude ratio of different components. Plotted synthetic waveforms have been aligned upon the MT inversion, with time shifts up to 6 s.

of 1.7 km and corresponds to a dominant positive isotropic source (49%), accompanied by steep east-southeast–west-northwest (33%) thrust faulting and positive CLVD (18%), with a magnitude estimate of M_w 4.86. The scalar moment is computed according to Silver and Jordan (1982). Noteworthy, the scalar moment of the isotropic term is slightly larger than the sum of the moment released by DC and CLVD, whereas the decomposition indicates an isotropic percentage of 49%. The isotropic MT has a magnitude M_w 4.79. Our full MT result is slightly larger but compatible with the full MT solution proposed by Ford *et al.* (2009) for the 2009 explosion, and also the estimated scalar moment ($1.7–2.2 \times 10^{16}$ N·m, considering isotropic or full MT scalar moments) is similar to the estimate of 1.5×10^{16} N·m (M_w 4.8), based on the waveform amplitude ratio for the January 2016 and 2009 events and the 2009 full MT scalar moment by Ford *et al.* (2009). The comparison of displacement waveforms is shown in Figure 3. Using other velocity models, we obtain slightly worse fits. Interestingly, the

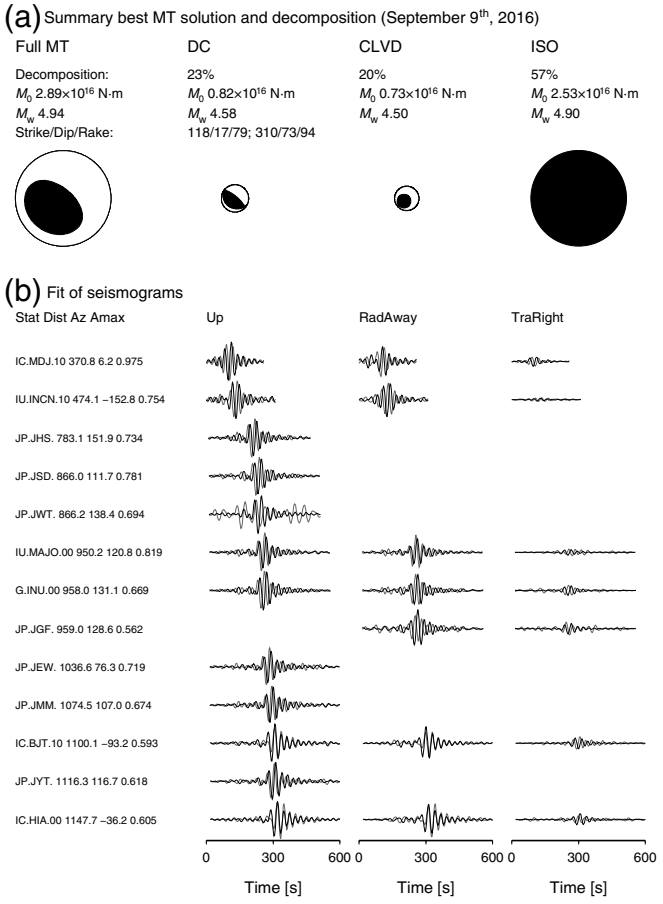

▲ **Figure 4.** MT inversion results for the 9 September 2016 explosion. (a) Summary of the best MT result out of the regional full-waveform amplitude spectra (up to 1200 km distance) MT inversion, with the polarity and centroid location constrained upon full-waveform displacements (up to 600 km distance). The plot reports the focal sphere of the full MT and decomposed terms, according to the standard decomposition, scalar moment, moment magnitudes, and orientation of the DC focal planes. (b) Fit of displacement traces in the time domain for the best MT solution. Synthetics are denoted by black thin lines and observations by gray thick lines. The network, station, location codes, the distances (km), the azimuth (°), and the maximal amplitudes (10^{-6} m) are reported at the left side. Traces are normalized according to the maximal amplitude at each station to highlight the amplitude ratio of different components. Plotted synthetic waveforms have been aligned upon the MT inversion, with time shifts up to 6 s.

resulting MT also shows some very different results, for example, with the inversion based on the CRUST model predicting an MT solution more compatible with the one proposed by Barth (2014) for the 2013 event (smaller isotropic term, northeast–southwest normal faulting and negative vertical CLVD). The differences among MT results for the January 2016 explosion using different earth models further extend the variability among MT solutions proposed for the 2009 and 2013 events.

The September 2016 explosion was larger in magnitude, as already shown by its larger waveform amplitudes (Fig. 2). MT inversion results and waveform fits are illustrated in Figure 4. The best MT solution is found at 1.8 km depth and decomposed into a dominant positive isotropic component (57%), a northwest–southeast steep thrust faulting (23%), and a positive CLVD (20%). The overall moment is 2.89×10^{16} N·m (M_w 4.94) and is mostly attributed to the isotropic component (scalar moment 2.53×10^{16} N·m, M_w 4.90). The MT decomposition is similar to the January explosion, but the DC term has an opposite steep dip angle.

MT INVERSION: UNCERTAINTIES AND TRADE-OFFS

To investigate possible ambiguities and MT resolution limits, we adopt a new MT inversion algorithm, able to identify MT solutions that reproduce the observation reasonably well. Objectives of this analysis are the estimation of MT uncertainties and the identification of source parameters trade-offs. The data and fitting procedure are very similar to those adopted for the previous MT inversion. The optimization algorithm is based on a simulated annealing approach (see the Ⓔ electronic supplement). The following source parameters are simultaneously resolved: centroid time, centroid location (latitude, longitude, depth), and six independent MT components. Other parameters, such as scalar moment, moment magnitude, and MT decomposition, can be directly derived. We discuss the results for the January 2016 event.

We first compute synthetics and spectra using model MDJ2 and discuss all solutions with an acceptable misfit, considering those not exceeding the minimum misfit (defined as L2 norm) by more than 10%. Results (Fig. 5) show a variety of acceptable solutions, ranging in the source decomposition space from the case of a dominant isotropic term to a dominant negative vertical CLVD. Among the first group of solutions, some are compatible with the full MT by Ford *et al.* (2009) and our standard amplitude spectra MT inversion result. The second group of solutions (large negative CLVD components) is compatible with the deviatoric solution by Ford *et al.* (2009). However, many solutions are located between these two extreme cases, in the first quadrant of the Hudson plot. Among these solutions (positive isotropic plus negative CLVD), some are compatible with the solution of Barth (2014) for the 2009 earthquake. Results are compared with relative estimates for the January 2016 event, based on the other explosion (2009, 2013, and September 2016). Similar patterns are found assuming different velocity models (Fig. 6), with some differences. For example, assuming the CRUST 2.0 model, the space of acceptable solutions remains constrained within the first quadrant of the Hudson plot, showing solutions consistent with Barth (2014). The trade-off also affects the magnitude estimate, the source depth, the size, and the geometry of the DC term. Considering all velocity models, the magnitude variation is large, spanning from M_w 4.4, for strong negative CLVD, to M_w 4.9, for a dominant isotropic term. Depth estimates vary between 0 and 2.5 km. The variation of the size and geometry of the DC term can be judged

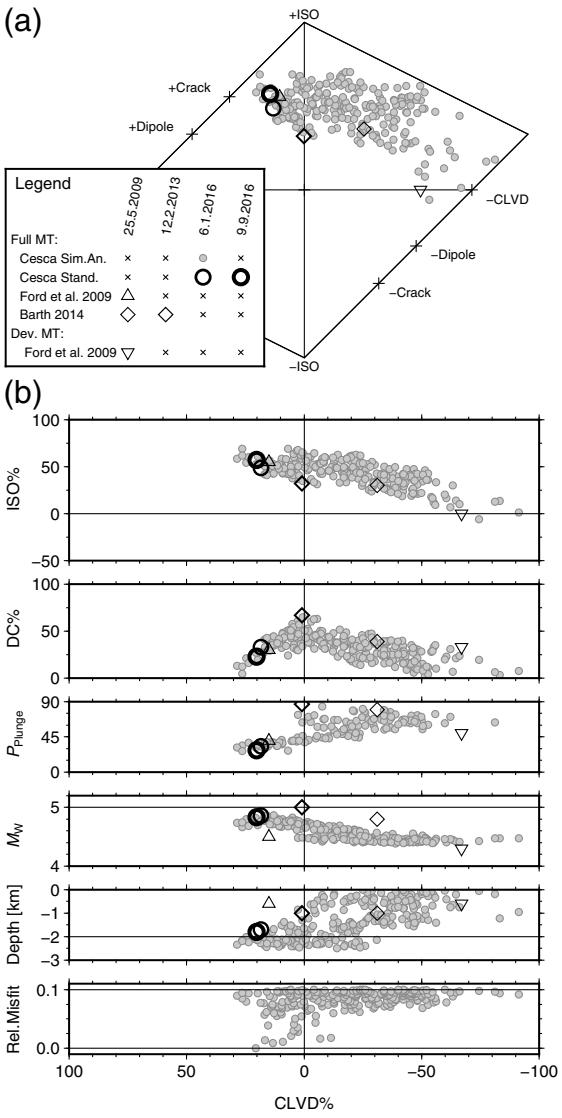

▲ **Figure 5.** (a) The source decomposition according to the Hudson source type diagram (Hudson *et al.*, 1989) illustrates the range of acceptable solutions for the regional MT inversion problem using the regional full waveforms of the January 2016 nuclear test, DPRK, and the MDJ2 velocity model (Ford *et al.*, 2009), ranging for high dominance of positive isotropic component (top in the plot) to high dominance of negative CLVD (right in the plot); the predicted range of solutions can explain the variability among solutions proposed for the 2009, 2013, and 2016 events by different authors (see legend for different symbols). (b) The lower plots illustrate the consequences of the strong trade-offs among MT entries, showing the resulting trends of isotropic percentage, DC percentage, pressure axis plunge (as an indicator of the fault-plane steepness and normal/thrust mechanism type) and moment magnitude (note that absolute and relative estimates are only for the January 2016 event) as a function of the CLVD percentage (plotted with the sign of its largest dipole). Note that magnitudes plotted with the 2009, 2013, and September 2016 symbols refer to the magnitude of the January 2016 event, as derived upon the original full MT moment estimate and the median scaling factor among vertical waveform amplitudes.

from Figure 5. The DC term is the largest when the CLVD is the smallest, dropping quicker for positive CLVD solutions (where the isotropic component is still large) than for negative CLVD ones. The pattern of the pressure (P) axis plunge reveals changes in the DC orientation: in correspondence to negative CLVD, the DC term is characterized by subvertical P axis, that is, normal faulting (mostly northeast–southwest striking, consistent with the DC models proposed by Barth, 2014); in contrast, solutions with an ~45° dipping P axis (steep thrust to vertical mechanism) are common in correspondence to dominant positive isotropic sources; these two extreme cases quite well resemble, respectively, the different DC terms resolved by Barth (2014) and Ford *et al.* (2009).

ARRAY BEAM MODELING

Although a best solution could be chosen upon a slightly better misfit, the former analysis points out important limitations in the robustness of the MT solution: choosing a slightly different velocity model or station configuration may easily lead to a different solution. To resolve the MT ambiguity, we make use of an independent observation, modeling the explosion signal at seismic arrays at teleseismic distances.

Three seismic arrays (Fig. 1) were originally considered in this study: GERES (Germany), ASAR (Alice Springs, Australia), and PDAR (Pinedale, Wyoming). They are located at different azimuths, respectively, northwest, south, and northeast of the epicenter, and at distances of 8189, 7210, and 8999 km. Vertical-component velocity seismic data from 24, 18, and 13 stations are downloaded from the three arrays, respectively. They are aligned based on calculated theoretical back azimuth (320°, 45°, and 356°) and slownesses (0.0528, 0.0589, and 0.0480 s/km, computed using the CRUST 2.0 velocity model at the source region) and stacked. The beam modeling part makes use of the QSEIS (Wang, 1999) reflectivity algorithm, taking into account independent source and receiver velocity models (upon the CRUST 2.0 database, Bassin *et al.*, 2000) and a common propagation model (ak135, Kennett *et al.*, 1995). Synthetic and observed velocity traces are stacked, normalized, band-pass filtered (1–6 Hz), and compared assuming different MT solutions and source depths. Results are shown in Figure 6 for the ASAR (Alice Springs, Australia) and the GERES (Germany) arrays, the fit at PDAR (Pinedale, Wyoming) resulting less clear. A comparison of observed and synthetic first-motion polarities from the *P*-wave beams, under the assumption of two competing MT source models (either dominated by a positive isotropic term or a negative vertical CLVD one), is able to reveal the correct decomposition and provides an independent confirmation for the MT solution characterized by a dominant positive isotropic source (Fig. 7). The best modeling results (Fig. 8), able to reproduce the waveform complexity, characterized by the overlap of *P* and *pP* onsets, is found for about 1.5 km, supporting the estimate of a shallow hypocenter.

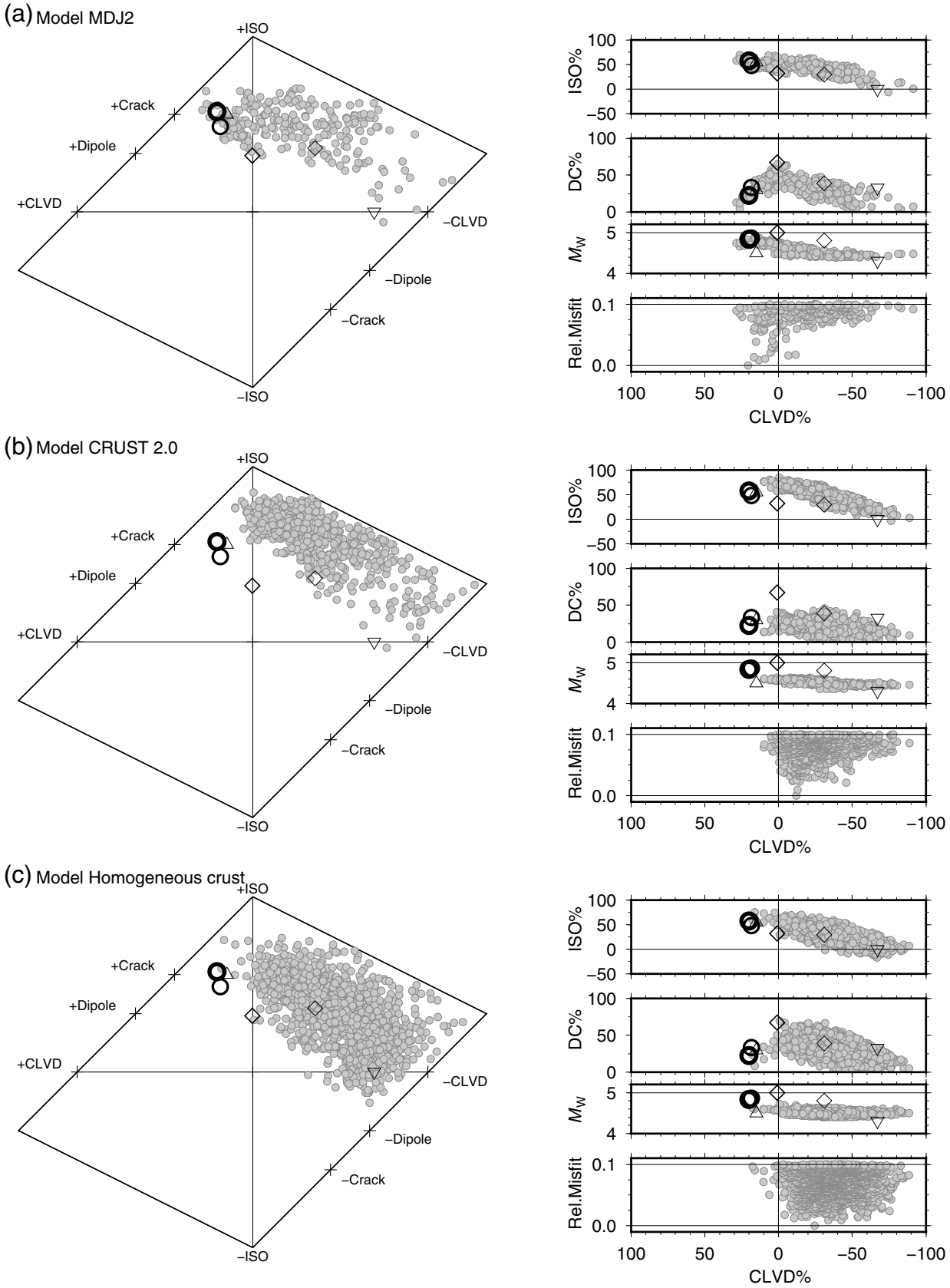

▲ **Figure 6.** Comparison of MT results for three velocity models: (a) MDJ2 after Ford *et al.* (2009), (b) CRUST 2.0 model for the epicentral region after Bassin *et al.* (2000), and (c) a homogenous crustal model derived from the CRUST 2.0 model. For each velocity model, the Hudson plot is shown on the left side and the distribution of isotropic (ISO) and DC percentage, moment magnitude, and relative misfits as a function of the CLVD percentage on the right side. Symbols and magnitude definition are the same as in Figure 5.

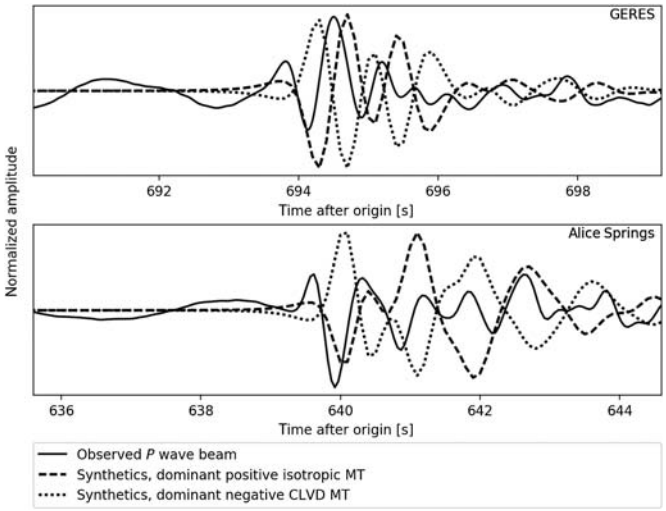

▲ **Figure 7.** Comparison of observed (solid line) and synthetic vertical *P*-wave displacement array beams at the GERES, Germany, and Alice Springs, Australia, seismic arrays for two competing source models: model 1 (dashed line) was computed for the best MT solution out of the amplitude spectra inversion, model 2 (dotted line) corresponds to a competing MT, dominated by a negative CLVD.

DISCUSSION

The comparative analysis of the nuclear explosion signals from North Korea (2009, 2013, and 2016 episodes) sheds light on the differences among proposed source models. The range of acceptable solutions (Fig. 5) maps the uncertainty distribution affecting the MTs. The region of acceptable MT decomposition is broad and accounts for MT solutions proposed for previous explosions, beside their differences. Discussing solutions for previous explosions in the light of results obtained for the 2016 explosions is justified by the high waveform similarity (Fig. 2). We compared absolute magnitude estimates for the 2016 events, based on waveform modeling, and relative estimates, based on magnitudes estimated for previous explosions. Our results are in agreement with the relative value based on Ford *et al.* (2009) but underestimate magnitudes suggested by Barth (2014). The Hudson plot (Hudson *et al.*, 1989) representation (Figs. 5 and 6) helps explain the apparent discrepancy among different proposed MTs: all published solutions fall within the broad MT uncertainty region. Out of the many acceptable solutions, distributed in three quadrants of the Hudson plot, a relatively large number presents unusual decompositions, with a combination of isotropic and CLVD terms of opposite signs. At the edges of this region, solutions close to positive isotropic and negative vertical CLVD could correspond to physical models of explosions and collapses, respectively. Solutions proposed by Barth (2014) and Ford *et al.* (2009) for the 2009 and 2013 events can be explained in the light of the existing trade-offs.

The ambiguity in the MT resolution mostly originates by the trade-offs among the trace components. Horizontal dipoles

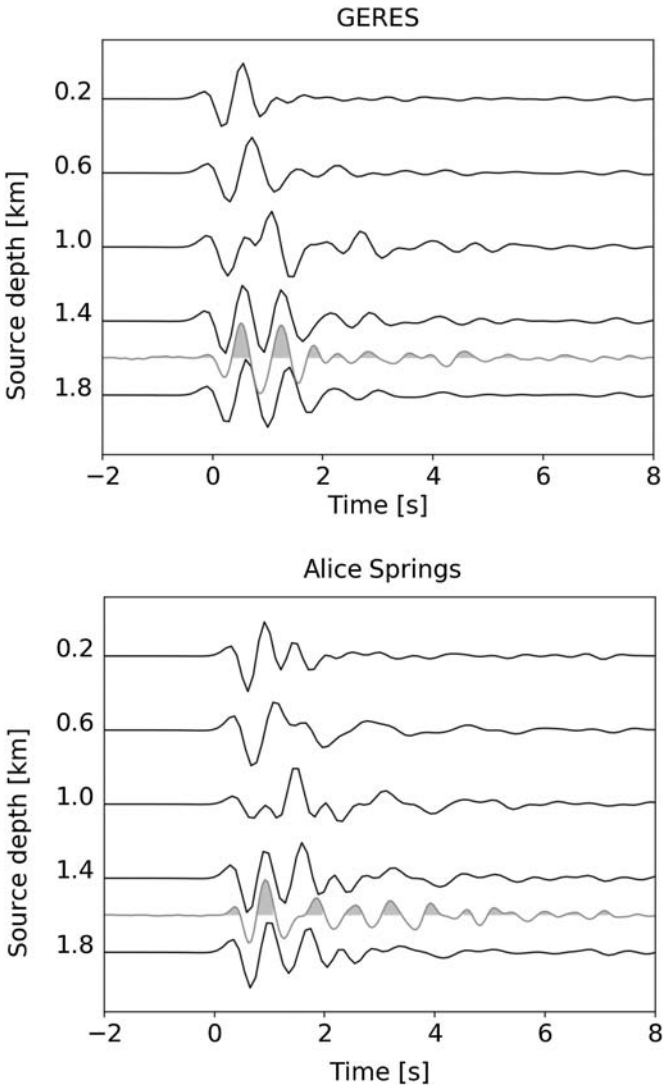

▲ **Figure 8.** Comparison of synthetic vertical *P*-wave array beams (black lines) computed for different source depth and observations (gray lines) at (a) the GERES, Germany and (b) Alice Springs, Australia, seismic arrays. Waveforms are aligned so that time 0 corresponds to the first *P* onset.

(M_{xx} and M_{yy}) present similar values for all solutions; the trade-off among horizontal and vertical MT dipoles is responsible for the trade-off among isotropic and CLVD terms. This ambiguity, combined with the depth trend, additionally affects the magnitude estimate. The correlation among depth and magnitude was already discussed in Ford *et al.* (2009).

It could be questioned whether the large differences among published solutions for previous explosions can be explained by the adoption of different velocity models by different authors. The effect of velocity model on MT inversion (e.g., Domingues *et al.*, 2013) was also considered here (Fig. 6). Although some differences are found among the solutions adopting different crustal models, the MT ambiguity is partially intrinsic and cannot be easily solved, even with an accurate velocity model. To prove this, we show how the trade-offs

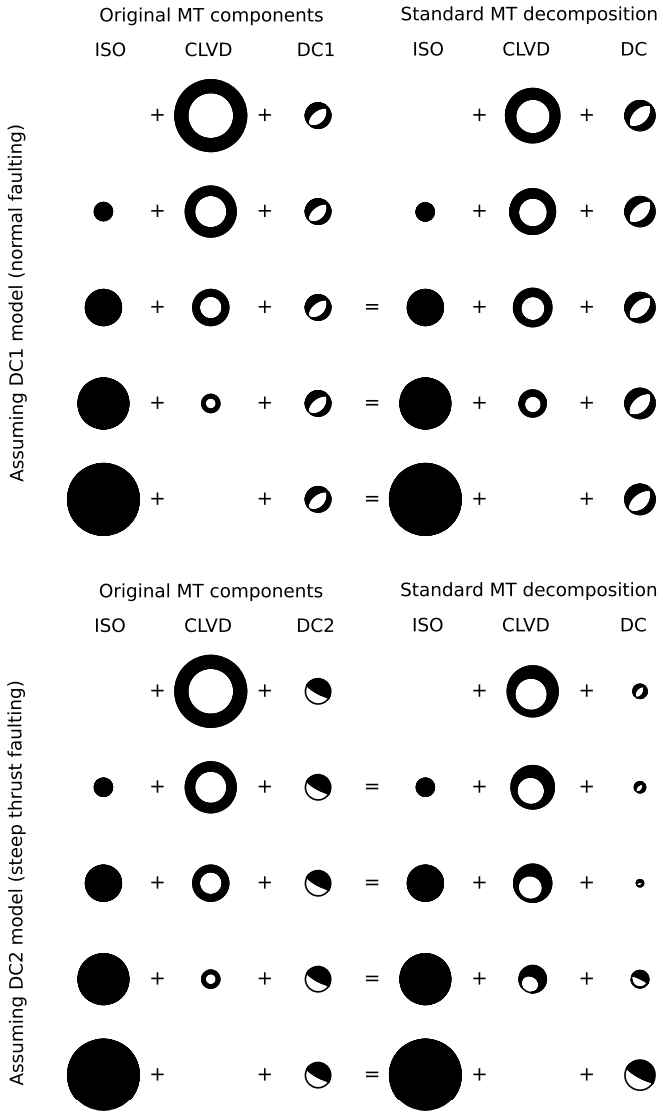

▲ **Figure 9.** Comparison of MT configurations poorly resolved using low-frequency full waveforms modeling at regional distances and assuming a shallow source. The original MT components (left side) are combinations of positive isotropic and negative vertical CLVD terms with different ratios. In addition, we consider a DC term, either assuming DC1 (top panel), which is a northeast–southwest normal faulting according to Barth (2014), or DC2 (bottom panel), which is a steep northwest–southeast thrust faulting, according to results of this study. The standard decomposition is unable to reconstruct the original configuration, especially when the DC and negative CLVD do not have common orientations for the pressure axis. As a result, the decompositions associated with DC2 can easily reproduce both original DC models, when assuming different ratios of the CLVD and DC components. Focal sphere areas are proportional to scalar moments.

among trace MT entries, scalar moment, and centroid depth can be reproduced using a controlled synthetic data inversion. We use a noise-free synthetic dataset, generated for a purely isotropic source, a known realistic velocity model (MDJ2), real stations configurations, and the same MT inversion setup used for the analysis of real data. Inversion results (see Ⓔ electronic supplement) prove that the synthetic data can be satisfactorily modeled by a weaker, shallower, negative vertical CLVD source. The isotropic-CLVD ambiguity mostly stems from the poor resolution of the M_{zz} component and its trade-off with the horizontal dipoles (see Ⓔ Fig. S3): interestingly, in this synthetic test, the true solution (poor positive isotropic) is at the edge of the cloud of well-fitting solutions, which extends in the Hudson plot toward a negative vertical CLVD.

A pure isotropic source cannot explain all seismic observations, in particular the low-amplitude transversal components. For the January 2016 and 2009 events, the deviatoric term is well modeled by an east-southeast–west-northwest very steep thrust faulting (see previous results and full MT solution by Ford *et al.*, 2009). For the September 2016 event, it has a similar strike but opposite dip angle. An alternative deviatoric source model (Barth, 2014, for the 2009 explosion) is a combination of northeast–southwest normal faulting and vertical negative CLVD. The variation of the DC term for different acceptable MT configurations is both consequence of MT uncertainties and MT decomposition. When the CLVD component is large, it controls the orientation of a weaker DC term. In the case of a negative CLVD, the standard decomposition forces the DC and CLVD to have a common pressure axis; in the current case, a strong vertical negative CLVD can force a 45° dipping normal faulting. When the DC term is larger than the CLVD, the DC will control the orientation of the CLVD term. To illustrate this ambiguity (Fig. 9), we consider two hypothetical DC terms: DC1 is a northeast–southwest normal faulting according to the solution of Barth (2014), whereas DC2 is a northwest–southeast steep thrust faulting as in our solution for the January 2016 explosion, which is also compatible with the results of Ford *et al.* (2009). We already discussed how positive isotropic and negative vertical CLVD solutions are hardly distinguishable, because they produce similar synthetic waveforms. Therefore, the ambiguity remains, when we add the contribution of a common DC term. In Figure 9, we consider different contributions of the CLVD and DC terms: five equivalent models are illustrated in different rows (in the upper plot for model DC1, and in the bottom plot for model DC2). When considering the DC1 model, because both the DC and CLVD terms have a negative vertical pressure axis, the standard decomposition of the resulting deviatoric MT is consistent with the original contributions. However, when considering the sum of DC2 and a vertical negative CLVD, the decomposition varies significantly, depending on the size of the DC2 and CLVD contributions. When the scalar moment associated with the DC term is larger, the MT decomposition correctly reveals the original northwest–southeast thrust faulting DC. When, in contrast, the CLVD is larger, then the decomposition of the deviatoric MT provides a normal faulting, perpendicular to the strike of the original DC2 thrust mechanism. Considering that the uncertainty affecting the isotropic-CLVD ratio, this model can explain all proposed MT solutions.

MT misinterpretation following the standard decomposition has been recently discussed by Rudzinski *et al.* (2016) and Heimann *et al.* (2015) for mine and volcanic caldera collapse events. The synthetic inversion proves the ambiguity in the resolution of regional full-waveform MT for a shallow source, which persists even when the velocity model is known. Seismic noise and the adoption of a specific velocity model can further affect the inversion with real data.

The discrepancy among the two deviatoric MTs resolved for the January and September 2016 events can be discussed in a similar manner. The two models are different but produce similar synthetic waveforms. As discussed in Figure 9 for one of them, they are undistinguishable from a combination of vertical negative CLVD and normal faulting, except for minor differences in the oblique components. Thus, it remains unresolved whether the deviatoric terms associated with the two explosions were really different or simply not resolved.

A potential reason behind the appearance of a residual nonisotropic term could be given by unmodeled wave propagation effects. However, such a lateral anomaly should similarly affect the waveforms for all explosions, because they took place in a reasonably compact region. The different characterization of transversal components for different explosions, with very similar waveforms but different azimuthal distribution of the relative amplitudes, rules out propagation effects as the origin for the nonisotropic terms. Their origin should be linked, instead, to near-source interactions. The activation of a neighboring fault, as proposed by Barth (2014) should also be excluded upon similar consideration, because the reactivation of a common fault would reveal compatible transversal components for different explosions. Our interpretation is that the nonisotropic term originates by a near-source interaction, possibly with a local topography feature or with the geometry of the tunnel system where the nuclear bombs were exploded.

The exploration of the source parameters' space illustrates other limitations of the MT inversion for the 2016 nuclear explosion. For example, the source depth remains very poorly resolved. The seismic array high-frequency beam modeling for *P*, *pP*, and *sP* phases could help resolve the focal depth. This method resulted here to be beneficial in verifying the MT solution and in resolving the isotropic-CLVD ambiguity; a comparison of observed and synthetic first-motion polarities from the *P*-wave beams, under the assumption of two competing MT source models (either dominated by a positive isotropic term or a negative vertical CLVD one), is able to reveal the correct decomposition.

Although the present case study may represent an extreme case, for which proven trade-offs strongly affect the MT solution interpretation and source parameter determination, the MT uncertainties can also affect the interpretation of MT inversion results for natural earthquakes. A careful quantification of MT components' uncertainties and identification of source parameters trade-offs provide a safe approach toward a robust MT interpretation.

CONCLUSION

We verified that regional and teleseismic signals originating from the nuclear explosions of 2016 are compatible with an explosive source, estimating a magnitude of M_w 4.8 and 4.9 for the isotropic sources of the January and September 2016 events (M_w 4.9 for the full MT solutions). A comparison of the 2016 seismic signals with those recorded upon previous explosions in 2009 and 2013 illustrated an increased amplitude of vertical components, proving that the September 2016 explosion released a seismic moment about 3.44, 1.84, and 1.45 times larger than previous ones in 2009, 2013, and January 2016, respectively. The combination of MT inversion and depth-phases modeling has the potential to recognize a combination of isotropic source and shallow depth, which is relevant toward nuclear explosion monitoring, even when only relying on seismological data at regional and teleseismic distances, and in the lack of local data. Beside a dominant isotropic term, the full MT presents a nonisotropic contribution, modeled as a combination of steep east-southeast–west-northwest thrust or vertical faulting and positive CLVD. We attribute such source contribution to seismic-wave interactions with structural anomaly, topographic structures, or the underground facilities configuration in the vicinity of the explosion. The MT inversion, decomposition, and interpretation remain challenging. A careful analysis of these uncertainties and resolution trade-offs reveals that a range of other mechanisms can well reproduce the seismological observations. As a consequence, the MT decomposition, the contribution of DC, CLVD and isotropic term, the DC orientation, and the magnitude can be strongly affected. The range of well-fitting MTs samples the space of MT decomposition between two back-end cases: (1) a mechanism dominated by a positive isotropic component, accompanied by subvertical thrust faulting and residual positive CLVD, which is compatible with an explosion source, and (2) a mechanism dominated by a vertical negative CLVD, accompanied by normal faulting and a negligible isotropic term. The first model can be finally safely chosen, both because of the weak misfit improvement in modeling regional full waveforms and upon the additional modeling of *P*-wave beams at teleseismic distances. This ambiguity explains the discrepancy among MT solutions proposed for the 2009 and 2013 events, which all fall into the MT uncertainty region. In particular, although the MT solutions proposed by Ford *et al.* (2009) and Barth (2014) appear very different, they may be extremely difficult to distinguish on the basis of their similar synthetic waveforms. It is worth noting that the MT ambiguity strongly affects the interpretation of the explosion size, which is poorly resolved: for example, for the January 2016 explosion, MT solutions with magnitudes ranging between M_w 4.4 and 4.9 can fit the seismic data reasonably well.

DATA AND RESOURCES

Seismic data were collected by the Incorporated Research Institutions for Seismology (IRIS; https://service.iris.edu/, last

accessed September 2016) U.S. Geological Survey (USGS), GEOSCOPE, Institute of Geophysics, China Earthquake Administration, Japan Meteorological Agency seismic networks, GERES (Germany), ASAR (Alice Springs ARray, Australia), and PDAR (Pinedale, Wyoming) seismic arrays. Data were obtained from the IRIS and GEOFON Data Management Center using International Federation of Digital Seismograph Networks (FDSN) web services. Data were processed with pyrocko (http://emolch.github.io/pyrocko, last accessed August 2016), and figures prepared using pyrocko and Generic Mapping Tools (GMTs). Data on the 6 January 2016 North Korean nuclear explosion test are available at GEOFON real-time bulletin (http://geofon.gfz-potsdam.de/fdsnws, last accessed September 2016).

ACKNOWLEDGMENTS

Marius Kriegerowski is funded by the German Deutsche Forschungsgemeinschaft–International Continental Drilling Program and High-resolution Imaging of Swarm Systems (DFG-ICDP HISS) Project (CE 223/2-1). We are thankful to Editor Z. Peng, A. Barth, and an anonymous reviewer for their accurate reviews and suggestions.

REFERENCES

Barth, A. (2014). Significant release of shear energy of the North Korean nuclear test on February 12, 2013, *J. Seismol.* **18,** 605–615, doi: 10.1007/s10950-014-9431-6.

Barth, A., F. Wenzel, and D. Giardini (2007). Frequency sensitive moment tensor inversion for light to moderate magnitude earthquakes in eastern Africa, *Geophys. Res. Lett.* **34,** L15302, doi: 10.1029/2007GL030359.

Bassin, C., G. Laske, and G. Masters (2000). The current limits of resolution for surface wave tomography in North America, *Eos Trans. AGU* **81,** F897.

Bukchin, B., E. Clévédé, and A. Mostinsky (2010). Uncertainty of moment tensor determination from surface wave analysis for shallow earthquakes, *J. Seismol.* **14,** 601–614.

Cesca, S., and F. Grigoli (2015). Full waveform seismological advances for microseismic monitoring, *Adv. Geophys.* **56,** 169–228, doi: 10.1016/bs.agph.2014.12.002.

Cesca, S., A. Rohr, and T. Dahm (2013). Discrimination of induced seismicity by full moment tensor inversion and decomposition, *J. Seismol.* **17,** 147–163, doi: 10.1007/s10950-012-9305-8.

Domingues, A., S. Custodio, and S. Cesca (2013). Waveform inversion of small-to-moderate earthquakes located offshore southwest Iberia, *Geophys. J. Int.* **192,** no. 1, 248–259, doi: 10.1093/gji/ggs010.

Dufumier, H., and L. Rivera (1997). On the resolution of the isotropic component in moment tensor inversion, *Geophys. J. Int.* **131,** no. 3, 595–606.

Ford, A. R., D. S. Dreger, and W. R. Walter (2009). Source analysis of the Memorial Day explosion, Kimchaek, North Korea, *Geophys. Res. Lett.* **36,** L21304, doi: 10.1029/2009GL040003.

Gilbert, F. (1971). Excitation of the normal modes of the earth by earthquake sources, *Geophys. J. Roy. Astron. Soc.* **22,** no. 2, 223–226, doi: 10.1111/j.1365-246X.1971.tb03593.x.

Heimann, S., S. Cesca, M. Hensch, V. Hjörleifsdóttir, E. Holohan, E. Rivalta, and T. Dahm (2015). Complex rupture processes at the Bardarbunga caldera, Iceland, *26th IUGG General Assembly*, Prague, Czech Republic, 22 June–2 July 2015.

Hudson, J. A., R. G. Pearce, and R. M. Rogers (1989). Source type plot for inversion of the moment tensor, *J. Geophys. Res.* **94,** no. B1, 765–774, doi: 10.1029/JB094iB01p00765.

Jost, M. L., and R. B. Hermann (1989). A student's guide to and review of moment tensors, *Seismol. Res. Lett.* **60,** 37–57.

Kawakatsu, H. (1996). Observability of the isotropic component of a moment tensor, *Geophys. J. Int.* **126,** 525–544.

Kennett, B. L. N., E. R. Engdahl, and R. Buland (1995). Constraints on the seismic velocities in the earth from travel times, *Geophys. J. Int.* **122,** 108–124.

Minson, S. E., and D. S. Dreger (2008). Stable inversion for complete moment tensors, *Geophys. J. Int.* **174,** no. 2, 585–592, doi: 10.1111/j.1365-246X.2008.03797.x.

Rudzinski, L., S. Cesca, and G. Lizurek (2016). Complex rupture process of the 19 March 2013, Rudna Mine (Poland) induced seismic event and collapse in the light of local and regional moment tensor inversion, *Seismol. Res. Lett.* **87,** no. 2A, doi: 10.1785/0220150150.

Shuler, A., G. Ekström, and M. Nettles (2013). Physical mechanisms for vertical-CLVD earthquakes at active volcanoes, *J. Geophys. Res.* **118**, no. B4, 1569–1586, doi: 10.1002/jgrb.50131.

Silver, P. G., and T. H. Jordan (1982). Optimal estimation of scalar seismic moment, *Geophys. J. Int.* **70,** no. 3, 755–787, doi: 10.1111/j.1365-246X.1982.tb05982.x.

Wang, R. (1999). A simple orthonormalization method for stable and efficient computation of Green's functions, *Bull. Seismol. Soc. Am.* **89,** no. 3, 733–741.

Wen, L., and H. Long (2010). High-precision location of North Korea's 2009 nuclear test, *Seismol. Res. Lett.* **81,** no. 1, 26–29.

Zhang, M., and L. Wen (2013). High-precision location and yield of North Korea's 2013 Nuclear Test, *Geophys. Res. Lett.* **40,** 2941–2946.

Simone Cesca
Sebastian Heimann
Joachim Saul[2]
Torsten Dahm
GFZ German Research Centre for Geosciences Potsdam
Telegrafenberg
14473 Potsdam, Germany
simone.cesca@gfz-potsdam.de
heimann@gfz-potsdam.de
saul@gfz-potsdam.de
torsten.dahm@gfz-potsdam.de

Marius Kriegerowski[1]
Institute of Earth and Environmental Sciences
University of Potsdam
Karl-Liebknecht Street 24-25
14476 Potsdam-Golm
Potsdam, Germany
marius@gfz-potsdam.de

Published Online 11 January 2017

[1] Also at GFZ German Research Centre for Geosciences Potsdam, Section 2.1 Physics of Earthquakes and Volcanoes, Helmholtzstrasse 7, 14467 Potsdam, Germany.

[2] Also at GFZ German Research Centre for Geosciences Potsdam, Section 2.4 Seismology, Telegrafenberg, 14473 Potsdam, Germany.